Journal of
Advanced Microscopy Research
Vol. 5, 137–142, 2010

Towards the Determination of Surface Energy at the Nanoscale: A Further Assessment of the AFM-Based Approach

Dimitrios A. Lamprou[1], James R. Smith[1], Thomas G. Nevell[1], Eugen Barbu[1], Colin R. Willis[2], and John Tsibouklis[1,*]

[1] *Biomaterials and Drug Delivery Group, School of Pharmacy and Biomedical Sciences, University of Portsmouth, St. Michael's Building, White Swan Road, Portsmouth PO1 2DT, UK*
[2] *Physical Sciences Department, Dstl Porton Down, Salisbury SP4 0JQ, UK*

Towards the validation of the atomic force microscopy-based approach to the determination of surface energy at the nanometer scale, this paper explores the applicability of the technique by comparing atomic force microscopy-derived surface energy values with those from conventional contact angle measurements from a range of self-assembled organosilane structures ((3-aminopropyl)triethoxysilane, (3-glycidoxypropyl)trimethoxysilane, 3-(triethoxysilyl)propylsuccinic anhydride and trimethoxy(propyl)silane) and also from films of an ultra-low-surface-energy polymer, poly(1H,1H,2H,2H-perfluorodecyl methacrylate). The close agreement between the two sets of data indicates the validity of the AFM method, while unique attributes are indicated by the high resolution (*ca.* 1000 atoms) that is inherent to the approach and by the capability to study materials that are not compatible with the probing liquids used for goniometric determinations.

Keywords: Surface Energy, Atomic Force Microscopy, Organosilanes, Goniometry.

1. INTRODUCTION

Surface energy (γ; γ_S), a measure of the mutual affinity of interacting surfaces,[1–3] is of key importance in applications that are as diverse as bioadhesion, adsorption and catalysis.[4–7] This parameter is normally determined from liquid-on-solid contact angle measurements (θ, the internal angle of a tangent drawn at the boundary between a liquid droplet in contact with a solid surface; contact angle goniometry, CAG) [8–11] that demand the use of liquids that do not penetrate the surface; resolution is limited by the size of the droplet and by surface roughness.

Recent work has detailed the first comparative study of the atomic force microscopy (AFM) and CAG methods for determining γ.[12] The AFM technique has been used to probe, in air, well defined alkanethiol self-assembled structures that had been attached to cleaned, gold-coated AFM tips and substrates.[13–14] For all alkanethiol self-assembled structures considered, values of interfacial energy (γ_{TM}) were found to be in close agreement with those from CAG measurements. Towards the assessment of the breadth of the applicability of the technique, this paper compares the AFM-determined γ values of a range of organosilane multilayer structures[15–17] and also of a dip-coated polymeric film with those from CAG experiments.

2. MATERIALS AND METHODS

2.1. Preparation of Glass Substrates and AFM Cantilevers

Glass microscope slides (Agar Scientific, Essex, UK; 1 mm thick) were cut into 1.25 cm × 1.25 cm coupons and cleaned using Piranha Solution (3:1 concentrated sulphuric acid, 33% (v/v): 30% hydrogen peroxide; Fisher Scientific, Loughborough, UK) for 30 min.[18] AFM cantilevers (silicon nitride, NP-20 'C' V-shaped cantilevers; Veeco Instruments SAS, Dourdan, France) and clean substrates were rinsed (water, Millipore, 16.5 MΩ cm) and dried (nitrogen) (Piranha Solution was found to damage AFM cantilevers).[13]

2.2. Silanisation of Glass Substrates and AFM Cantilevers

Organosilanes, (3-Aminopropyl)triethoxysilane (APTES, 99%, NH_2-terminated; Acros Organics, Geel, Belgium),

*Author to whom correspondence should be addressed.

(3-glycidoxypropyl)trimethoxysilane (GPTMS, 97%, epoxy-terminated; Alfa Aesar, Heysham, UK), 3-(triethoxysilyl) propylsuccinic anhydride (TESPSA, 95%, CO_2H-terminated; Wacker-Chemie GmbH, Burghausen, Germany) and trimethoxy(propyl)silane (TPS, 98+%, CH_3-terminated; Alfa Aesar, Heysham, UK), Figure 1, were grafted onto AFM cantilevers and onto cleaned glass surfaces by immersion into a solution of the silane (APTES, 5% (v/v); TESPSA, 10% (v/v); TPS, 20% (v/v); GPTMS, 20% (v/v)) in toluene (99%; Fisher Scientific, Loughborough, UK).[17] The effect of immersion time on surface energy was investigated at specified time intervals over a period of 32 h. To promote surface relaxation in silane structures and to remove physisorbed multilayers,[17, 19] silanised glass surfaces were subjected to sequential sonications in toluene, N,N-dimethylformamide (DMF, 99%; Sigma, Steinheim, Germany) and ultrapure water (20 min each), and dried (nitrogen) before use. Prior to sonication, and irrespective of chemical structure, CAG-determined surface energies of organosilanes on glass (16 h immersion) were 54 ± 3 mJ m^{-2}; those on Piranha-cleaned glass were 43 ± 2 mJ m^{-2}.

2.3. Polymer-Coated Surfaces and AFM Cantilevers

Gold-coated glass microscope slides (Au.1000.ALSI, Platypus Technologies, Madison, Wisconsin, USA, cut to 1.25 cm × 1.25 cm) and gold-coated AFM cantilevers (NPG-20 'C' V-shaped cantilevers; Veeco Instruments SAS, Dourdan, France) were cleaned by immersion in Gold Surface Cleaning solution (thiourea 1% (w/v) in 10% aqueous sulphuric acid; Sigma-Aldrich, Poole, UK; 1 h and 5 min, respectively), rinsed (water, Millipore, 16.5 MΩ cm) and dried (nitrogen).[13] Immediately after cleaning, gold-coated substrates and cantilevers, and glass substrates and silicon nitride cantilevers were immersed in poly(1H,1H,2H,2H-perfluorodecyl methacrylate) (PFDMA; 5% in 1,1,2-trichlorotrifluoroethane, 99.8%, Aldrich, Dorset, UK)[20] for 1 min.

2.4. Contact Angle and Surface Energies

To probe liquid-surface interactions at maximal resolution, contact angles (θ at 20 °C) of small drops (×4 on each substrate) of diiodomethane ('DIM', >99%, surface tension $\gamma_L = 48.7$ mN m^{-1} at 18.8 °C, lit.[21] = 50.76 mN m^{-1} at 20 °C; *ca.*1 μL) and 1,2-ethanediol (ethylene glycol, 'EG', >99%; $\gamma_L = 47.7$ mN m^{-1} at 18.8 °C, lit.[21] = 48.40 mN m^{-1} at 20 °C; *ca.*1 μL), Sigma-Aldrich, Poole, UK, and water ('FW,' filtered, $\gamma_L = 73.4$ mN m^{-1} at 18.8 °C, lit.[21] = 73.05 mN m^{-1} at 18.0 °C; *ca.* 2 μL; pH = 5.6) placed on horizontal substrates (×2) were measured using a goniometer with an enclosed thermostated cell (Kruss G10, Hamburg, Germany). Advancing (θ_A) and receding (θ_R) angles (±0.1°; with syringe needle removed to enable curve fitting of drop-shape image) were obtained for both 'left' and 'right' contact angles at 20–30 s after placement of the drop.[4] Surface energies of substrates (γ_s) were calculated from the contact angles and the interfacial energies (γ_l) of the three probe liquids from Eqs. (1), (2)[22, 23] using a Visual Basic program (University of Portsmouth).

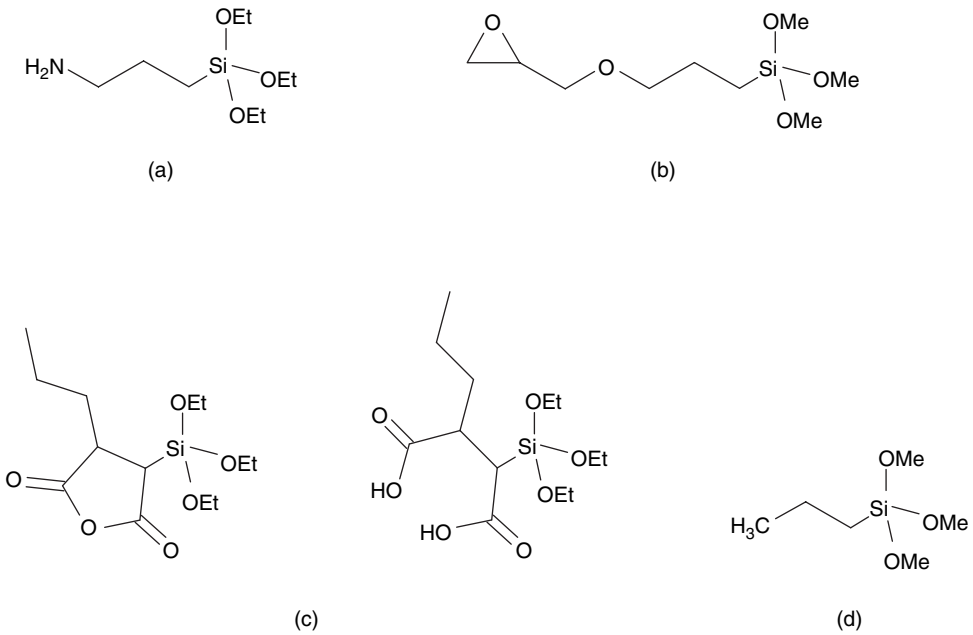

Fig. 1. (a) (3-Aminopropyl)triethoxysilane (APTES), (b) (3-glycidoxypropyl)trimethoxysilane (GPTMS), (c) 3-(triethoxysilyl)propylsuccinic anhydride (TESPSA) and hydrolysis product, and (d) trimethoxy(propyl)silane (TPS).

$$\gamma_s = \gamma_s^{LW} + \gamma_s^{AB} = \gamma_s^{LW} + 2\left(\gamma_s^+\gamma_s^-\right)^{0.5} \quad (1a)$$

$$\gamma_l = \gamma_l^{LW} + \gamma_l^{AB} = \gamma_l^{LW} + 2\left(\gamma_l^+\gamma_l^-\right)^{0.5} \quad (1b)$$

$$\gamma_l(1+\cos\theta) = 2[(\gamma_s^{LW}\gamma_l^{LW})^{0.5} + (\gamma_s^+\gamma_l^-)^{0.5} + (\gamma_s^-\gamma_l^+)^{0.5}] \quad (2)$$

where superscripts denote components of surface energy: Lifshitz-van der Waals LW, acid-base AB, Lewis acid γ^+ and Lewis base γ^- (in mJ m^{-2}: FW, $\gamma_l^{LW} = 21.8$, $\gamma_l^+ = \gamma_l^- = 25.5$; DIM, $\gamma_l^{LW} = 50.8$, $\gamma_l^+ = \gamma_l^- = 0$; EG, $\gamma_l^{LW} = 29$, $\gamma_l^+ = 1.92$, $\gamma_l^- = 47$).[24]

Water contact angles of silanised surfaces were also measured at pH 2.5 (0.1 mol dm^{-3} potassium hydrogen phthalate (100 mL) in 0.1 mol dm^{-3} HCl (77.6 mL)), pH 7.5 (0.1 mol dm^{-3} KH_2PO_4 (100 mL) in 0.1 mol dm^{-3} NaOH (82.2 mL)), and pH 12.5 (0.2 mol dm^{-3} KCl (50 mL) in 0.2 mol dm^{-3} NaOH (40.8 mL)), to investigate the effects of pH on θ.

2.5. Atomic Force Microscopy

A MultiMode/NanoScope IV Scanning Probe Microscope (Digital Instruments, Santa Barbara, CA, USA; Veeco software Version 6.11r1) was used for AFM measurements in air (temperature 22 ± 1 °C; relative humidity 40 ± 2% and 55 ± 1% for the silanes and polymers, respectively). Force versus distance plots were obtained using silicon nitride probes (NP-20 'C' V-shaped cantilevers; nominal length (l_{nom}) = 115 μm, width (w_{nom}; measured perpendicular to long axis) = 17 μm, resonant frequency (υ_{nom}) = 56 kHz, spring constant (k_{nom}) = 0.32 N m^{-1}; Veeco Instruments SAS, Dourdan, France) and the J-scanner (maximum *xyz*-translation = 200 × 200 × 16 μm^3). The laser alignment was unaltered during measurements (deflection sensitivity = 65 ± 15 nm V^{-1}) and arrays of 10 × 10 force-curves (lateral separation, 100 ± 5 nm; ramp size, 800 nm; scan rate, 1.03 Hz) were produced from ten different areas (1000 nm × 1000 nm, separated by 1000 nm) on each surface. Measurements were repeated twice using silane surfaces that had been formed sequentially onto glass substrates and F_{ad} values were extracted from force curve data using an in-house-developed Visual Basic program. An accurate value of k (Eq. (3)[25]) was obtained from measurements by scanning electron microscopy (JSM-6060LV, JEOL Ltd, Japan; 10 and 25 keV, 35 μm spotsize, working distance 12–14 mm) of the thickness t, length l and width w of the cantilever (Effective Young's modulus E = 175 GPa)[26], Table I.

$$k = \frac{Et^2w}{2l^2} \quad (3)$$

F_{ad} is related to the work of adhesion (W_{ad}) using either the Johnson-Kendall-Roberts (JKR) theory[27] or Derjaguin-Muller-Toporov (DMT) theory[28], Eq. (4):

$$\gamma_{SM} = \gamma_{TM} = \frac{1}{2}W_{ad} = \frac{F_{ad}}{2c\pi R} \quad (4)$$

Table I. Measured values of tip radius R, cantilever thickness t, length l, width w and calculated values of k for each cantilever used (Effective Young's modulus E = 175 GPa).[26]

Tip SD	R/nm ±1	l/μm ±0.1	w/μm ±0.1	t/μm ±0.02	υ/kHz ±0.5	k/N m^{-1} ±0.02
Silicon nitride	89	97.5	17.1	0.58	55.0	0.31
TESPSA	75	110.2	18.2	0.58	60.0	0.26
GPTMS	78	112.9	18.9	0.59	52.4	0.25
APTES	77	111.9	17.2	0.58	48.4	0.23
TPS	90	115.7	18.9	0.58	49.0	0.23
PFDMA (NP)	80	111.9	19.9	0.58	61.1	0.24
PFDMA (NPG)	76	108.5	16.5	0.58	65.5	0.22

where c = 1.5 and 2 respectively for JKR and DMT models, and γ_{SM} and γ_{TM} are interfacial energies.

The tip radius (R) for each AFM tip was determined by scanning, in contact mode (scan size 4 μm, scan rate 1.03 Hz), an etched silicon surface that possessed features that were sharper than R (TGT01; MikroMasch, San Jose, CA, USA). The radius of curvature was determined by drawing a line-profile across a tip artefact and exporting the height versus width data into an in-house Visual Basic program that allowed the manual fitting of a circle to the tip shape. Surface roughness (R_a) was determined by entering surface scanning data (contact mode, NP-20 'C' cantilever; 2 areas on 2 reformed surfaces, scan size = 5 μm, scan rate = 1 Hz) into a digital leveling algorithm (Veeco Image Analysis software V 7.10).

3. RESULTS AND DISCUSSION

3.1. Organosilanes Deposited onto Glass

To determine the optimum immersion time required for organosilane coverage, γ_s (CAG) was monitored for glass surfaces that had been exposed to silane solutions (5–20% v/v in toluene) for specified periods (1–32 h, Fig. 2). Surface energy values corresponded with those expected on the basis of the chemical nature of the terminal groups: CO_2H > epoxy > NH_2 > CH_3 (GPTMS > TESPSA > APTES > TPS; Fig. 2); and, water contact angles (Table II) agreed broadly with literature values for silanes on Si wafers (TESPSA, 27.2 ± 5.1°;[19] GPTMS, 44.3 ± 1.6° [19] and 52°;[29] APTES, 41.6 ± 2.8° [19] and 60°;[30] TPS, 82.4°).[31] Since for all silane structures γ_s values had been found to be reproducible for samples that had been immersed in the parent solution for 16 h, the immersion time for all silanisation reactions was set at 16 h.

Since silanes on glass are more stable than corresponding alkanethiol SAMs on gold, it has been proposed that they are more suitable for uses as biomedical materials.[32] To assess the effects of pH variation on the surface energy of implantable silane structures, θ_A and hysteresis

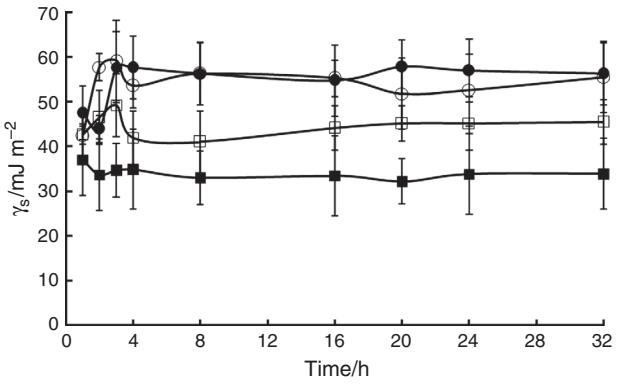

Fig. 2. Surface energies (γ_s) as calculated from advancing (θ_A) and receding (θ_R) average contact angles on organosilanes grown on glass following different immersion times ($n = 2$; $T = 22$ °C): (○) = TESPSA, (●) = GPTMS, (□) = APTES, (■) = TPS.

(θ_{Hys}) values of silane-functionalised glass substrates have been measured at three biologically relevant pHs, namely: pH 2.5, 7.5 and 12.5 (Table II).

The θ_A of the glass surface (control) was seen to decrease with increasing pH; the low θ_{Hys} values are consistent with a surface that is flat and homogeneous, as expected. Glass is similar to amorphous silica, in that silanol group coverage has been estimated at *ca.* 4.5 SiOH groups nm^{-2}.[33] These groups become either positively or negatively charged, depending on pH (point of zero charge = pH 2–3;[34,35] pK$_a$ (SiOH groups) = 5 – 7[36,37]), explaining the effect of pH on θ_A.

For the TESPSA surface, θ_A increased with increasing pH (from $33 \pm 3°$ to $46 \pm 1°$ for pH 2.5 and pH 7.5) but at pH 12.5 θ_A dropped to below the measurable limit of our instrument ($\theta < 15°$), as expected and in accord with the based catalysed hydrolysis of the ester anhydride functionality and the possible deprotonation of the resulting dicarboxylic acid structure. This behaviour is consistent with observations on the variation of pH on a carboxylic acid-terminated polyethylene surface.[38] GPTMS exhibited only a small pH-dependent reduction in θ_A, which is consistent with the expected Lewis base behaviour of the epoxide ring structure; the increase in θ_{Hys} with increasing pH must however reflect some protonation-induced surface modification. Consistent with the acid-induced quaternisation of the amino functionality, APTES exhibited similar θ_A values ($36 \pm 4°$ and $37 \pm 4°$) at pH 2.5 and 7.5, but θ_A decreased to $< 15°$ at pH 12.5; APTES is positively charged up to pH 10.2, the pK$_a$ value of the conjugate acid,[39] but above this pH value the amphoteric amine functionality becomes a proton donor allowing the surface to acquire a negative charge which in turn accounts for the low θ_A value. Large θ_{Hys} values associated with this surface are reflective of considerable heterogeneity: it is known that only 30–50% of silanol groups are grafted during silanisation.[40] As expected, the θ_A and θ_{Hys} values characterising the relatively inert TPS surface were little affected by pH.

With the exception of TPS structures, the F_{ad} values characterising the interaction between each of the silanised glass substrates and an uncoated silicon nitride tip were similar (*ca.* 90 nN vs. *ca.* 40 nN for TPS; Fig. 3), with the implication that these values must reflect the combined effects of the polarity of the silanised layer and the extent of hydrogen bonded interactions between the interacting surfaces.[41] The F_{ad} values for the silanes are less differentiated than γ_s values obtained from CAG (Fig. 2).

Using similarly silanised AFM tips and substrate surfaces, γ_{TM} values were obtained from W_{ad} measurements (Eq. (4), Table III). TESPSA and GPTMS had relatively high values (JKR: 52 ± 3 mJ m^{-2} and 50 ± 3 mJ m^{-2}, respectively), as expected due to their high polarity. The lower γ_{TM} for APTES (JKR: 41 ± 3 mJ m^{-2}) may be due to the presentation of methylene groups into the surface or due to interactions of the NH_2 groups with the glass/polar silane matrix.[30,42–44] TPS exhibited a similar γ_{TM} value that was higher than that expected for a hydrophobic tail group, as assessed by comparing the determined value

Table II. Water advancing (θ_A) and receding (θ_R) contact angles, and hysteresis (θ_{Hys}) values of silanated glass at different pH (2.5, 7.5 and 12.5); $n = 8$ (4 droplets on each of duplicate substrates); 16 h.

	Water contact angles, θ/°								
	pH 2.5			pH 7.5			pH 12.5		
Surface	θ_A	θ_R	θ_{Hys}	θ_A	θ_R	θ_{Hys}	θ_A	θ_R	θ_{Hys}
Glass	47 ± 4	45 ± 5	2	38 ± 5	33 ± 2	5	29 ± 1	27 ± 1	2
TESPSA	33 ± 3	32 ± 2	1	46 ± 1	40 ± 1	6	—*	—*	—*
GPTMS	44 ± 1	42 ± 1	2	38 ± 3	32 ± 4	6	34 ± 4	27 ± 2	7
APTES	36 ± 4	29 ± 1	7	37 ± 3	26 ± 2	11	—*	—*	—*
TPS	79 ± 4	76 ± 3	3	81 ± 3	79 ± 3	2	77 ± 5	75 ± 5	2

*$\theta < 15°$ (could not be measured with the available instrument).

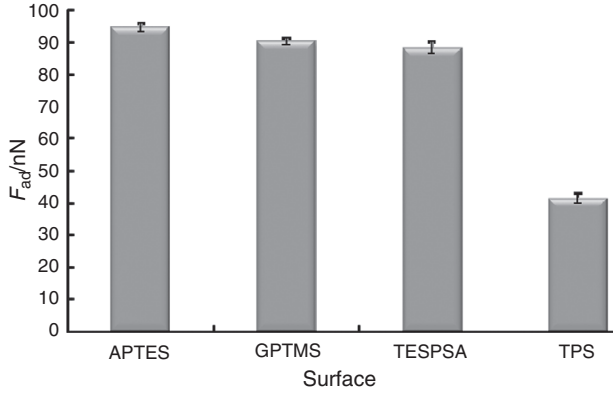

Fig. 3. Force of adhesion (F_{ad}) values for the interaction between a silicon nitride AFM tip and each organosilane (air; $n = 2$; 16 h).

Table III. Determined values of F_{ad}, W_{ad} and R_a for organosilane-coated glass substrates and tips ($T = 22 \pm 1$ °C, $RH = 40 \pm 2\%$; 10 areas, 10×10 force measurements for each), and corresponding surface energies, γ_{TM}, from JKR and from DMT calculations.

System	F_{ad}/nN	R_a/nm	W_{ad} (JKR)/mJ m^{-2}	W_{ad} (DMT)/mJ m^{-2}	γ_{TM} (JKR)/mJ m^{-2}	γ_{TM} (DMT)/mJ m^{-2}
TESPSA–TESPSA	36 ± 2	1.5	103 ± 7	77 ± 5	52 ± 3	39 ± 2
GPTMS–GPTMS	37 ± 2	2.7	99 ± 5	75 ± 3	50 ± 3	37 ± 2
APTES–APTES	30 ± 2	0.8	81 ± 6	61 ± 4	41 ± 3	30 ± 2
TPS–TPS	38 ± 2	0.9	87 ± 4	66 ± 3	43 ± 3	33 ± 2

with that seen for corresponding 1-undecanethiol SAM-tip interactions on gold (JKR: 32 ± 3 mJ m^{-2}).[12] This may be explained in terms of the inefficiency of the relatively short hydrophobic chains (C_3) to mask the influence of the extensive polar silane matrix and/or in terms of the increased disorder in multilayered films. The γ_S values obtained from θ_A and θ_R (CAG) measurements are in close agreement with γ_{TM} (JKR) values from AFM experiments (Fig. 4) but, with the exception of the more non-polar silane structure, γ_{TM} (DMT) values are significantly lower (Fig. 4).

3.2. Poly(1H,1H,2H,2H-Perfluorodecyl Methacrylate)

The γ_s of PFDMA has been evaluated at 12.7 ± 0.7 mJ m^{-2} (JKR) or at 9.5 ± 0.6 mJ m^{-2} (DMT) using both gold-coated AFM tips (NPG) and glass surfaces and at 7.9 ± 0.5 mJ m^{-2} (JKR) or at 5.9 ± 0.4 mJ m^{-2} (DMT) using silicon nitride tips (NP) and glass surfaces. The γ_{TM} (JKR) value determined with the NP-glass system is almost identical to the CAG-determined γ_s value for the same polymer on glass (7.5 ± 0.4 mJ m^{-2}).[20] Heterogeneous coverage of the polymer over the gold-coated substrate and/or the influence of interactions with the underlying gold may have had some effect on the reported evaluations.

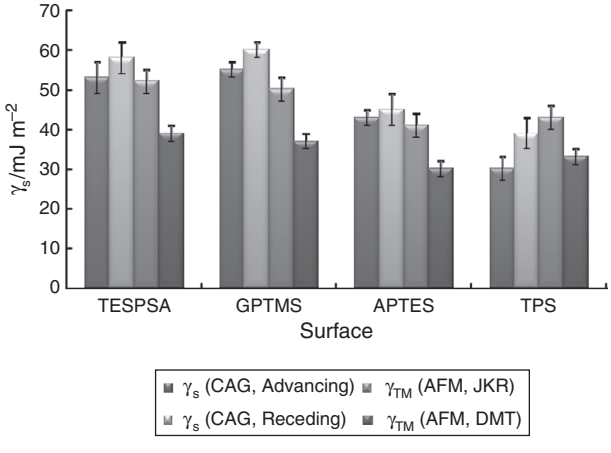

Fig. 4. Surface energies determined by CAG (θ_A and θ_R) versus AFM (JKR and DMT methods; $n = 2$; 16 h).

4. CONCLUSIONS

The capability of the atomic force microscope as a tool for the determination of surface energy has been demonstrated against a number of functionalised surfaces, providing further evidence that the technique may be universally applicable.

Acknowledgment: We thank the Institute of Biomedical and Biomolecular Sciences (IBBS), University of Portsmouth, for providing a studentship to DL.

References and Notes

1. W. M. Merrill, A. V. Pocius, B. V. Thakker, and M. Tirrell, *Langmuir* 7, 1975 **(1991)**.
2. J. C. Hooton, C. S. German, M. C. Davies, and C. J. Roberts, *Eur. J. Pharm. Sci.* 28, 315 **(2006)**.
3. J. Pacifico, K. Endo, S. Morgan, and P. Mulvaney, *J. Am. Chem. Soc.* 22, 11072 **(2006)**.
4. A. W. Adamson and A. P. Gast, Physical Chemistry of Surfaces, 6th edn., Wiley-Interscience, New York **(1997)**.
5. M. Graupe, T. Koini, H. I. Kim, N. Garg, Y. F. Miura, M. Takenaga, S. S. Perry, and T. R. Lee, *Colloids Surf.* 154, 239 **(1999)**.
6. V. J. Morris, A. R. Kirby, and A. P. Gunning, Atomic Force Microscopy for Biologists, Imperial College Press, London **(1999)**.
7. C. I. Pereni, Q. Zhao, Y. Liu, and E. Abel, *Colloids Surf. B: Biointerfaces* 48, 143 **(2006)**.
8. A. W. Neumann and R. J. Good, *Surf. Colloid Sci.* 11, 31 **(1979)**.
9. R. G. Good and C. J. van Oss, Modern Approaches to Wettability: Theory and Applications, edited by M. E. Schrader and G. Loeb, Plenum Press, New York **(1991)**, pp. 1–27.
10. A. Amirfazli and A. Neumann, *Adv. Colloid Interf. Sci.* 110, 121 **(2004)**.
11. T. Blake, *J. Colloid Interface Sci.* 299, 1 **(2006)**.
12. D. A. Lamprou, J. R. Smith, T. G. Nevell, E. Barbu, C. Stone, C. R. Willis, and J. Tsibouklis, *Appl. Surf. Sci.* 256, 5082 **(2010)**.
13. D. A. Lamprou, J. R. Smith, T. G. Nevell, E. Barbu, C. R. Willis, and J. Tsibouklis, *Appl. Surf. Sci.* 256, 1961 **(2010)**.
14. D. A. Lamprou, J. R. Smith, T. G. Nevell, E. Barbu, C. Stone, C. R. Willis, R. J. Ewen, and J. Tsibouklis, *Surf. Sci.* 604, 540 **(2010)**.
15. P. Silberzan, L. Leger, D. Ausserre, and J. J. Benattar, *Langmuir* 7, 1647 **(1991)**.
16. A. Ulman, An Introduction to Ultrathin Organic Films: From Langmuir-Blodgett to Self-Assembly, Academic Press, New York **(1991)**.
17. G. K. Toworfe, R. J. Composto, I. M. Shapiro, and P. Ducheyne, *Biomaterials* 23, 631 **(2006)**.
18. A.-S. Duwez, C. Poleunis, P. Bertrand, and B. Nysten, *Langmuir* 17, 6351 **(2001)**.

19. M. H. Lee, D. A. Brass, R. Morris, R. J. Composto, and P. Ducheyne, *Biomaterials* 26, 1732 **(2005)**.
20. J. Tsibouklis, P. Graham, P. J. Eaton, J. R. Smith, T. G. Nevell, J. D. Smart, and R. J. Ewen, *Macromolecules* 33, 8460 **(2000)**.
21. G. W. C. Kaye and T. H. Laby, Table of Physical and Chemical Constants, 15th edn., Longman Scientific and Technical, Harlow **(1992)**.
22. W. A. Zisman, Relation of the equilibrium contact angle to liquid and solid constitution, Contact Angle, Wettability, and Adhesion, edited by R. F. Gould, D.C. Advances in Chemistry Series 43, American Chemical Society, Washington **(1964)**, pp. 1–51.
23. J. Long, M. Hyder, R. Huang, and P. Chen, *Adv. Colloid Interface Sci.* 118, 173 **(2005)**.
24. B. Janczuk, T. Bialopiotrowicz, and A. Zdziennicka, *J. Colloid Interface Sci.* 221, 96 **(1999)**.
25. W. F. Stokey, Shock and Vibration Handbook, McGraw-Hill, New York **(1989)**.
26. L. L. Hazel and V. V. Tsukruk, *Thin Solid Films* 339, 246 **(1999)**.
27. K. L. Johnson, K. Kendall, and A. D. Roberts, *Proc. R. Soc. London A* 324, 301 **(1971)**.
28. B. V. Derjaguin, V. M. Muller, and Y. P. Toporov, *J. Colloid Interface Sci.* 53, 314 **(1975)**.
29. V. V. Tsukruk, I. Luzinov, and D. Julthongpiput, *Langmuir* 15, 3029 **(1999)**.
30. P. A. Heiney, K. Grueneberg, J. Fang, C. Dulcey, and R. Shashidhar, *Langmuir* 16, 2651 **(2000)**.
31. H. Onoe, K. Matsumoto, and I. Shimoyama (eds.), *Proc. 16th IEEE Annual Internat. Conf. Micro Electro Mechanical Systems*, Kyoto, Japan **(2003)**.
32. A. Kurella and N. B. Dahotre, *J. Biomater. Appl.* 20, 6 **(2005)**.
33. L. T. Zhuravlev, *Colloids Surf. A: Physicochem. Enging. Aspects* 74, 71 **(1993)**.
34. G. A. Parks, *Chem. Rev.* 65, 177 **(1965)**.
35. A. Carré, F. Roger, and C. Varinot, *J. Colloid Interface Sci.* 154, 174 **(1992)**.
36. M. L. Hair and W. Hertl, *J. Phys. Chem.* 74, 91 **(1970)**.
37. R. A. Van Wagenen, J. D. Andrade, and J. B. Hibbs, *J. Electrochem. Soc.* 123, 1438 **(1976)**.
38. S. R. Holmes-Farley, R. H. Reamey, T. J. McCarthy, J. Deutch, and G. M. Whitesides, *Langmuir* 1, 725 **(1985)**.
39. M. Bezanilla, S. Manne, D. E. Laney, Y. L. Lyubchenko, and H. G. Hansma, *Langmuir* 11, 655 **(1995)**.
40. E. F. Vansant, P. Van der Voort, and K. C. Vranken, Characterization and Chemical Modification of the Silica, Elsevier, Amsterdam **(1995)**.
41. H.-J. Butt, B. Cappella, and M. Kappl, *Surf. Sci. Rep.* 59, 1 **(2005)**.
42. W. J. Van Ooij and A. Sabata, Silanes and Other Coupling Agents, edited by K. L. Mittal, VSP International Science, The Netherlands **(1992)**, pp. 323–343.
43. K. M. R. Kallury, P. M. Macdonald, and M. Thompson, *Langmuir* 10, 492 **(1994)**.
44. E. W. Van der Vegte and G. Hadziioannou, *Langmuir* 13, 4357 **(1997)**.

Received: 8 June 2010. Accepted: 16 June 2010.